Harmonic Mitigation in a Hybrid Power System Integrated Shunt Active Power Filter Employing FLC and an Adaptive Current Control Technique

Pritam Patel[1], **Sarita Samal**[1], **Chitralekha Jena**[1], and **Prasanta Kumar Barik**[2†], Non-members

ABSTRACT

The main objective of this study is to mitigate current harmonic issues in hybrid renewable energy systems based on solar photovoltaic (SPV) and wind energy distribution. This is achieved with the help of a suitable controller-based shunt active power filter (SAPF). The SAPF is designed using a modified synchronous reference frame (MSRF) to reference current generation, an adaptive hysteresis current controller (AHCC) for switching pulse generation, and a fuzzy logic controller (FLC) for DC-link voltage regulation. The results of the proposed SAPF model developed in MATLAB/Simulink, show that the filter performs remarkably well in suppressing harmonics under different loading conditions. It is capable of fast corrective action under dynamic conditions and outperforms previous methods in terms of harmonic mitigation and dc-link voltage stabilization. The control techniques are compared on the basis of parameters such as harmonic compensation and dc-link voltage ripple reduction capability under changing load conditions. The results obtained through simulation represent the validity of the filter performance.

Keywords: Harmonics, Power Quality, Hybrid Power System, Solar Photovoltaic, Shunt Active Power Filter, Wind Energy System

1. INTRODUCTION

Energy is the life of the modern global economy and the underlying driving force by which society works. As the most vital form of energy, electricity is generally considered to be the backbone of modern civilization. Access to electrical power has become a basic human need like food, clothing, shelter, water, and clean air. Maintaining service reliability and being able to access good quality electrical power in terms of voltage, current, and frequency is generally referred to as electrical power quality (PQ).

Furthermore, the planet is currently in the grip of a massive power crisis. Conventional energy sources are not only scarce and costly but also harmful to the environment [1]. The modern world requires unrestricted access to clean, uncontaminated, and plentiful energy sources. Due to their inevitable benefits, governments around the globe are gravitating toward renewable sources. Renewable sources are safe for the environment, abundant in nature, and cost-effective [2]. Solar, wind, and fuel cells are examples of renewable sources [3].

Solar energy is very pure and freely available throughout the planet. It also has a lower carbon footprint and produces no greenhouse gases [4]. To increase its efficiency, the solar system must be linked to electronic equipment. The maximum power point tracking (MPPT) strategy is used to collect the most power from solar panels [5].

Wind energy is also environmentally friendly and emits no greenhouse gases and uses much less water than other energy sources [6]. Electricity generated by a wind power plant is less expensive than that provided by other sources [7]. The most effective wind energy solution (WES) consists of permanent magnet synchronous generator (PMSG)-based wind turbines with a fixed pitch angle [8]. The energy generated by the WES is first converted to dc and then fed to a boost converter through a diode rectifier. The system's power is optimized by using a boost converter with an MPPT controller. An inverter can be employed at the boost converter's terminals to give optimal power to three-phase customer loads [9]. The missing energy can be provided via a battery energy storage system [10] if the user load rises or the wind speed drops suddenly.

The combination of complementary renewable energy sources and conventional generators, a controller, power conditioning equipment, and an energy storage device is called a hybrid energy system. It is reliable, cost-effective, and eco-friendly. The nonlinear load drawing a non-sinusoidal current, creating harmful harmonic effects in a renewable energy distribution system, is now of great concern and the traditional passive filters have several drawbacks in the compensation of harmonics. Therefore, to find a dynamic and adjustable solution for harmonic mitigation, a Japanese group of power quality pioneers have developed an attractive and viable solution to power quality problems. Such equipment for harmonic

Manuscript received on April 28, 2022; revised on July 21, 2022; accepted on August 18, 2022. This paper was recommended by Editor-in-Chief Yuttana Kumsuwan.

[1]The authors are with the Kalinga Institute of Industrial Technology, Bhubaneswar, Odisha, India.

[2]The author is with the Department of Mechanical and Electrical Engineering, Odisha University of Agriculture and Technology, Bhubaneswar, Odisha, India.

[†]Corresponding author: prasantbarik05@gmail.com

Digital Object Identifier: 10.37936/ecti-eec.2023211.248667

mitigation is known as an active powerline conditioner or simply an active power filter (APF).

APFs are also employed for load balancing, flickering reduction, neutral current correction, and reactive power compensation, among other things [11]. APFs address the limitations of PFs with the use of switching devices. For harmonic current and reactive power adjustment, the shunt active power filter (SAPF) is linked to the point of common coupling (PCC) [12]. A variety of time domain-based control approaches for the SAPF, such as the instantaneous "p-q" theory method, synchronous reference frame (SRF), modified synchronous reference frame (MSRF) method, and so on are cited in [13].

SAPFs in current harmonic compensation, based on instantaneous reactive power theory and the SRF method, are applied in domestic, commercial, and industrial applications [14–16]. The design/simulation and experimental investigations on the SAPF for harmonics and reactive power compensation are carried out in [17]. In the majority of the existing literature, the generation of the theta angle method is implemented using basic SRF and modified SRF schemes, minimizing the inherent drawbacks of the SRF method [18]. Hence, in this work, the MSRF technique is implemented in the SAPF control algorithm. In this control stage, switching pulse width modulation (PWM) pulses are obtained by the error signals generated from the comparison between reference current and sensed actual currents. Various gating signal generation methods are reported in the literature.

In [19], the authors proposed a hysteresis current controller (HCC) based PWM current control method for generating pulses for SAPF. This method achieves constant switching and is easy to implement. However, the disadvantage of HCC is that the change in switch frequency is unequal within a specific band. An adaptive hysteresis current controller (AHCC) was designed in [20] to circumvent these constraints by adjusting the hysteresis band according to supply and load parameters to improve PWM inverter performance. Moreover, as explained in [21], the dc side voltage of SAPF should be regulated to ensure the transient stability of the distribution system. The DC side capacitor in SAPF is used to maintain the power balance in the system. If the load is suddenly increased, the capacitor discharges and delivers power to the load to achieve source and load power balance. Similarly, if the load is suddenly removed, the capacitor overcharges, maintaining power balance. To achieve this, the voltage across the DC side capacitor needs to be regulated. The DC voltage controller generates the desired charging current reference which is given to the inner current loop.

Following a disturbance in source or load, the DC voltage controller generates the desired shift of the reference current so that under transient conditions the SAPF also compensates for reactive and harmonic currents. In [9], the authors proposed a linear control method for regulating the DC side voltage of the SAPF. A PI controller is designed and implemented to control the DC voltage. The classic PI controller has a fixed gain value and produces high overshoot and time delay during transient conditions which degrade the effectiveness of the SAPF. The time-consuming tuning process and identifying the exact mathematical model are also drawbacks of the PI controller. Therefore, the fuzzy logic controller is more preferable than the PI controller [22–25]. A fuzzy logic controller is designed and implemented to control the DC voltage. Conventionally, the SAPF uses PI controllers to compute the active power losses and reactive power compensation control loops. Moreover, for better performance, the FLC is implemented in this study.

Following a review of the literature, the MSRF-based control methodology is used in this study for generating the reference signal, the AHCC technique for switching the signal, and the FLC for DC-link voltage control.

The key objectives of this study are as follows:

- To design a hybrid power system (HPS) comprising solar photovoltaic (SPV), a wind energy system (WES), and battery energy storage system (BESS) as an alternative energy source in MATLAB/Simulink environment.
- To design a DC-DC boost converter with a suitable MPPT controller for both SPV and WES in an HPS.
- To design a SAPF with different control schemes.
- To analyze and mitigate the PQ issue by integrating the proposed controller-based SAPF under inductive and capacitive type nonlinear loads.

This paper is organized as follows: the proposed HPS with an MPPT and boost converter is modeled in Section 2. The SAPF's setup and proposed control scheme are examined in Section 3 and Section 4. In Section 5, the suggested hybrid system is integrated with the SAPF for harmonic mitigation. The study finishes with a brief conclusion in Section 6.

2. HYBRID POWER SYSTEM MODEL

2.1 Modeling of the solar photovoltaic

Solar energy is very pure and freely available throughout the planet. It also has a lower carbon footprint and produces no greenhouse gases. Solar energy is a superb alternative source for electrical power generation because it is pollution-free and abundant in nature. The following section explains the specifics of the SPV system design.

2.2 Modeling of the solar panel

The proposed system uses a PV array as shown in Fig. 1, simulated using a model based on the existing literature. The nonlinear output characteristics of the SPV model are written as in Eq. (1), while the perturb and observe (P&O) MPPT flowchart is shown in Fig. 2. Table 1 contains the parameters of the SPV system. The boost converter design is shown in Fig. 3. The output DC voltage is determined using the duty ratio D. The SPV

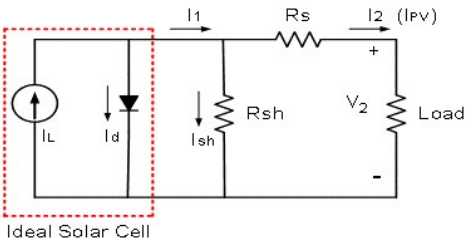

Fig. 1: Solar photovoltaic model.

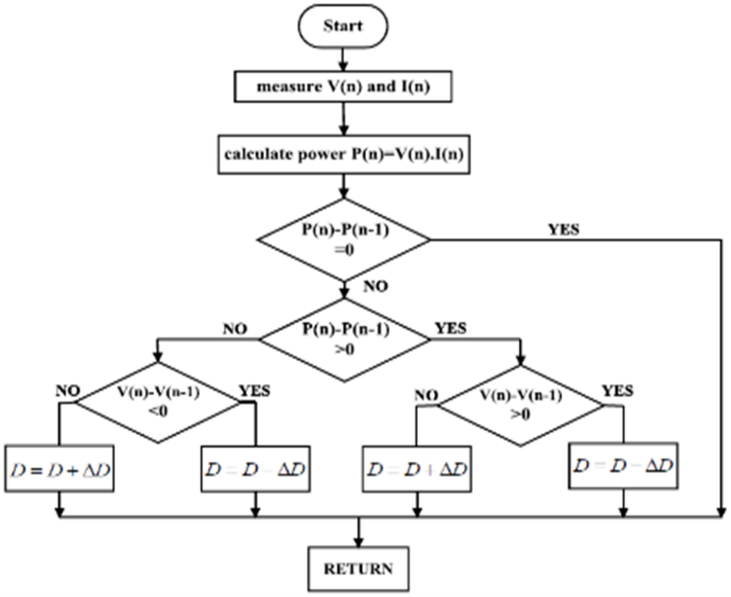

Fig. 2: MPPT flowchart.

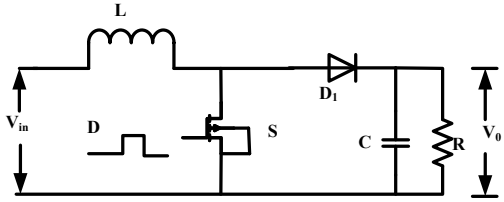

Fig. 3: Boost converter.

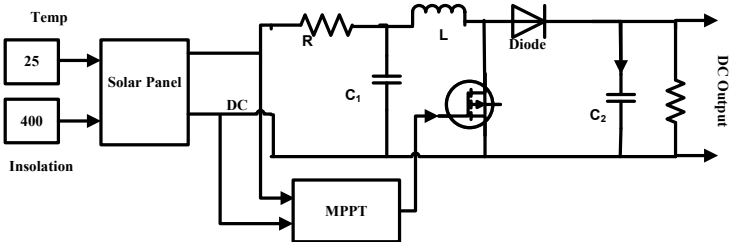

Fig. 4: SPV model with MPPT and boost converter.

***Table 1**: SPV system specifications.*

Parameters	Ratings
V_{mp}	81.5 V
I_{mp}	8.6 A
I_{sc}	10.2 A
V_{oc}	90.5 V
N_p	72
N_s	012
V_0	230 V

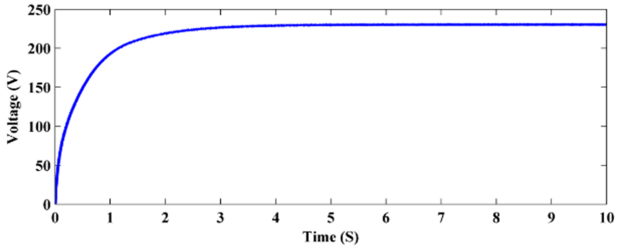

Fig. 5: Output waveform of SPV.

system with boost converter and MPPT is presented in Fig. 4, while Fig. 5 depicts the output voltage.

$$I_2 = I_L - I_0\left(e^{q(V_2+I_2R_s)/knT} - 1\right) - \left(\frac{V_2 + I_2R_s}{R_{sh}}\right) \quad (1)$$

2.3 Modeling of the wind energy system

In the hybrid source structure, the wind system is another distributed generator (DG). To generate energy, a PMSG-based WEC is implemented using Eq. (2). The fundamental WEC system is depicted in Fig. 6, while Figs. 7 and 8 show the overall model and output waveform.

$$P_0 = \frac{1}{2}\pi\rho C_P(\lambda,\beta)R^2V^3 \quad (2)$$

2.4 Modeling of the battery energy storage system

Batteries with electrical appliances store energy in an electric state, saving the extra energy for later use. In both solar and wind power systems, the battery bank has a switch connected to a standard DC bus with a constant voltage. Power transmission occurs with this DC bus at a constant voltage whether from a generator to a charger or battery bank or from a battery bank to a charger. Battery

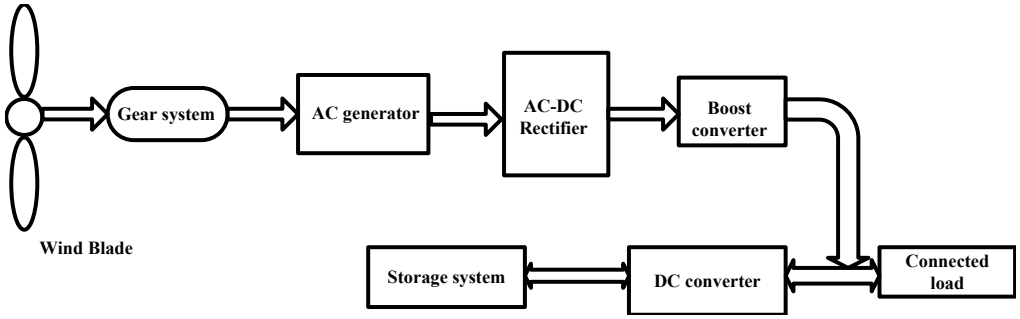

Fig. 6: Block diagram of the WES.

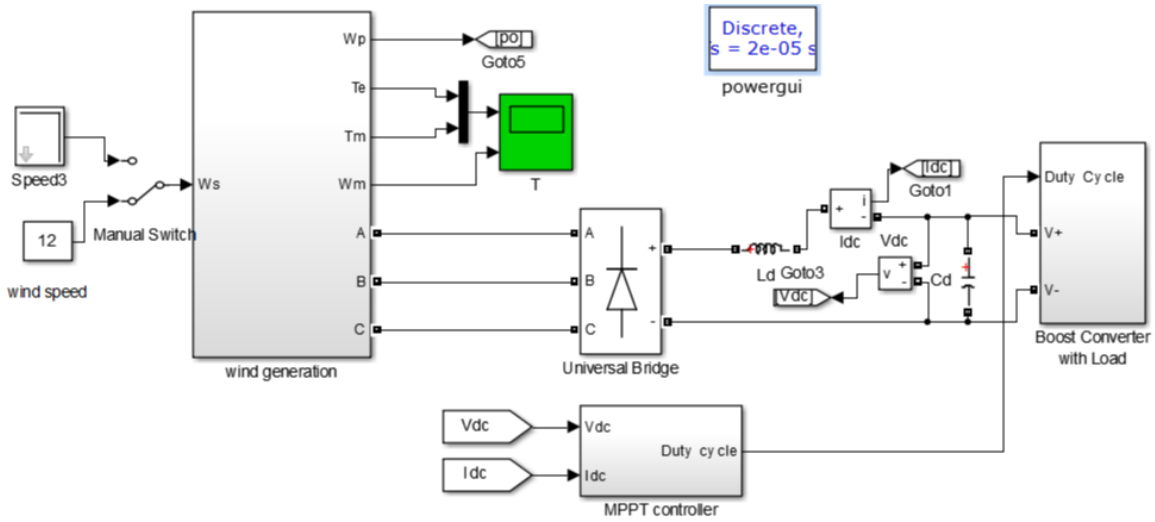

Fig. 7: Overall WES model.

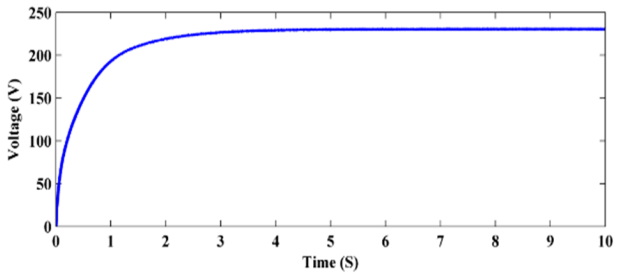

Fig. 8: Output waveform of WES.

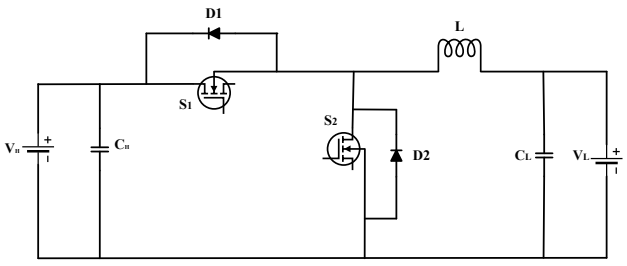

Fig. 9: Circuit diagram of the bidirectional converter.

power flow does not guide each route. Therefore, a bidirectional converter is required to create bidirectional power flow. It charges or discharges the battery during surplus and power outage conditions, respectively. The circuit diagram of the bidirectional converter is presented in Fig. 9.

3. DESIGN OF THE SHUNT ACTIVE POWER FILTER

3.1 Components of the Shunt Active Power Filter

To cancel out the harmonic currents of the nonlinear load and compensate for reactive power, the SAPF system responds by supplying/drawing a harmonic current to/from the supply. As a result, the current generated by the utility grid is sinusoidal and harmonic-free. Fig. 10 shows a block diagram of the SAPF.

3.1.1 VSI

To generate the compensating current, six insulated gate bipolar transistors (IGBTs) are employed to handle the charging and discharging of the DC-link capacitor. This converter's switching operation is entirely dependent on the control block design.

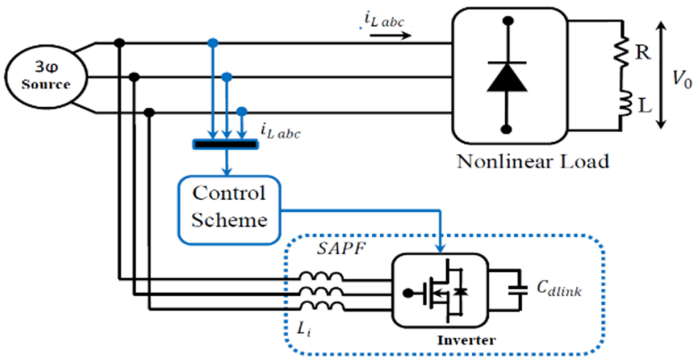

***Fig. 10**: Basic structure of SAPF.*

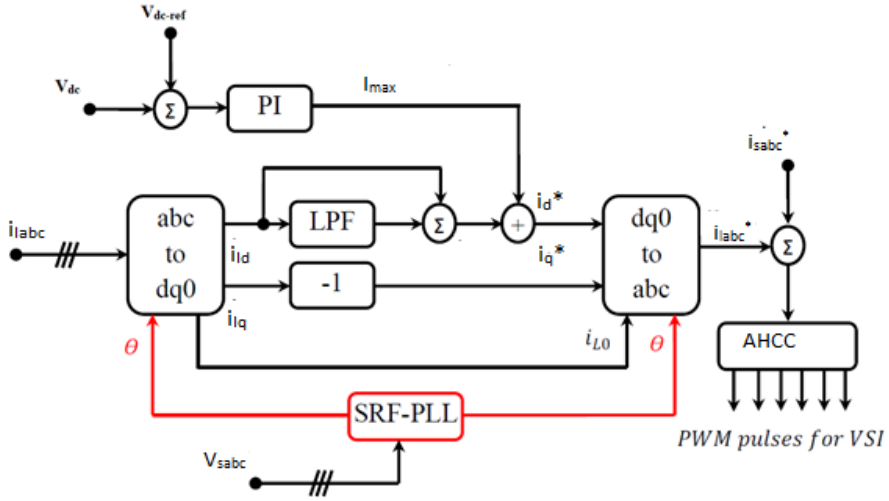

***Fig. 11**: SRF method.*

3.1.2 DC-Link Capacitor

This capacitor provides the load with the required reactive power. Large capacitors are typically used to maintain a steady DC voltage.

3.1.3 Control Block

The SAPF's overall performance is determined by the control block. The reference current and are used to create control signals for the power switches. The SAPF injects an appropriate amount of compensating current in the opposite phase of the harmonic current to eliminate harmonics from the source current (i_s).

The following fundamental equations are used to recognize the SAPF functionality.

$$i_c(t) = i_s(t) - i_l(t) \tag{3}$$

$$v_s(t) = V_s \sin \omega t \tag{4}$$

In the case of nonlinear load

$$i_l(t) = i_1 \sin\left(\omega t + \varphi_1\right) + \sum_{n=2}^{\infty} i_n \sin\left(n\omega t + \varphi_n\right) \tag{5}$$

where $i_s(t)$ is the source current, $i_l(t)$ is the load current, $i_c(t)$ is the compensating current, and φ_1 is the angle between the current and fundamental voltage.

4. SAPF CONTROL SCHEME

4.1 Reference Current Generation

4.1.1 SRF control technique

The basic SRF scheme model is revealed in Fig. 11, where the load current (i_{la}, i_{lb} and i_{lc}) and transfer to $i_d - i_q$ are acknowledged in Eq. (6).

$$\begin{bmatrix} i_{ld} \\ i_{lq} \\ i_{l0} \end{bmatrix} = \frac{2}{3} \begin{bmatrix} \cos\theta & \cos\left(\theta - \frac{2\pi}{3}\right) & \cos\left(\theta + \frac{2\pi}{3}\right) \\ -\sin\theta & -\sin\left(\theta - \frac{2\pi}{3}\right) & -\sin\left(\theta + \frac{2\pi}{3}\right) \\ \frac{1}{2} & \frac{1}{2} & \frac{1}{2} \end{bmatrix} \begin{bmatrix} i_{la} \\ i_{lb} \\ i_{lc} \end{bmatrix} \tag{6}$$

The load current is then passed via an low pass filter (LPF) to filter out the harmonic components, leaving only the fundamental component. Finally, the inverse park-transformation approach is used to convert this current to a three-phase stationary frame.

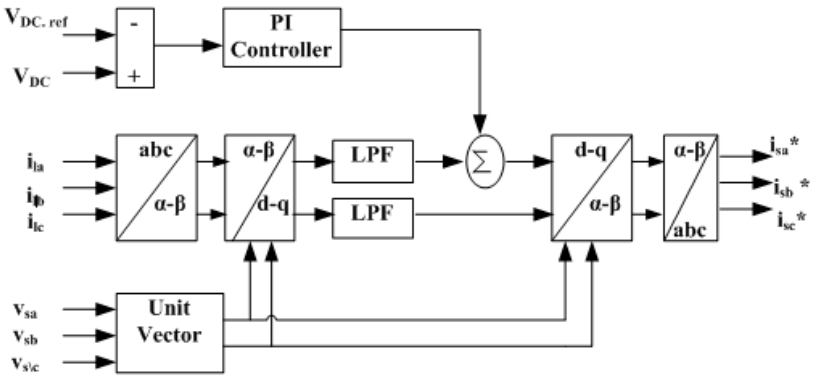

Fig. 12: MSRF-based control scheme.

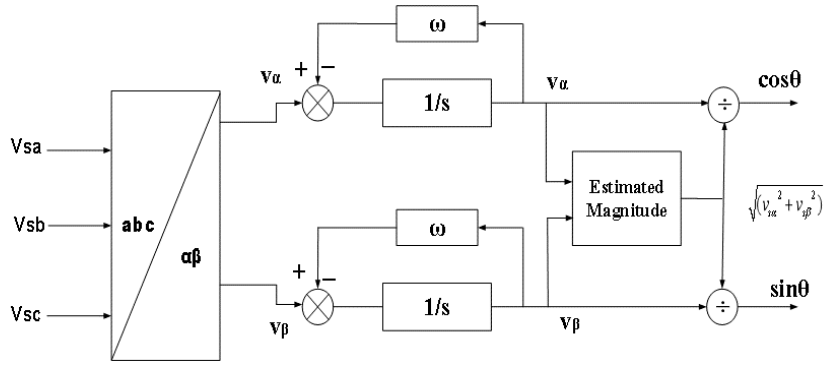

Fig. 13: Unit vector generation technique.

4.1.2 MSRF method

Instead of using a phase-locked loop (PLL) circuit like in the SRF approach, the MSRF method uses a simplified unit vector generating scheme to accomplish synchronization [19]. Fig. 12 shows a block diagram of the MSRF design. In this scheme, the synchronization angle is fed as an input for the transformation of concerned signals (v_s) to $\alpha - \beta$ reference frame (i.e. $V_{s\alpha}$ and $V_{s\beta}$). Thereafter, LPFs are used to reduce the voltage harmonics of the corresponding signals. A block diagram of the reference current generation scheme is shown in Fig. 13. The process for generating the θ angle is defined in Eqs. (7) and (8).

$$\cos\theta = \frac{V_\alpha}{\sqrt{\left(V_{s\alpha}{}^2\right) + \left(V_{s\beta}{}^2\right)}} \tag{7}$$

$$\sin\theta = \frac{V_\beta}{\sqrt{\left(V_{s\alpha}{}^2\right) + \left(V_{s\beta}{}^2\right)}} \tag{8}$$

4.2 Generation Scheme for Switching Pulses

Due to its simplicity, the HCC current control technique is chosen for this study.

4.2.1 HCC Scheme

Many methods have been documented in the literature, but the HCC strategy has proven to be more advantageous for the SAPF. Fig. 14 shows the HCC's detailed control mechanism in action.

4.2.2 AHCC Scheme

Due to the drawbacks of the fixed-band HCC mentioned above, AHCC is proposed in this study since it builds the hysteresis bandwidth, calculated instantaneously according to the compensation current variation and voltage, hence the switching speed becomes smooth and the frequency switching fixed considerably. According to the system topology presented in Fig. 15, the relationship between the hysteresis band (HB) and f_s is presented by Eq. (9).

$$HB = \frac{0.125V_{dc}}{f_s L_i}\left[1 - \frac{4L_i^2}{V_{dc}^2}\left(\frac{V_s}{L_i} + \frac{di_{sa}^*}{dt}\right)\right] \tag{9}$$

where f_s is the modulation frequency.

4.3 DC side Voltage Regulation

The SAPF is connected primarily to inject i_c into the PCC, lowering the harmonic content and necessary

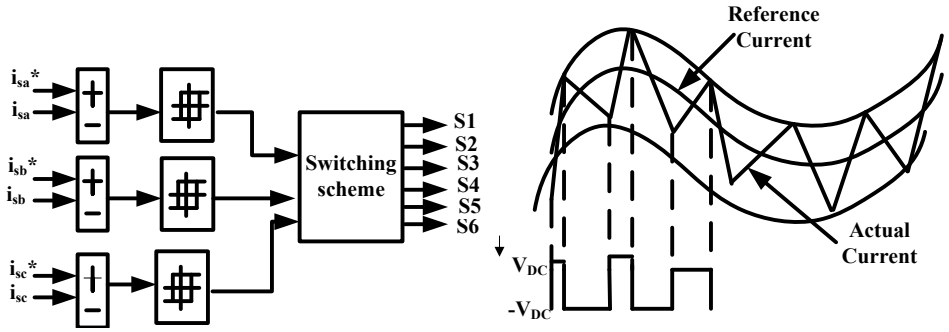

Fig. 14: HCC switching scheme.

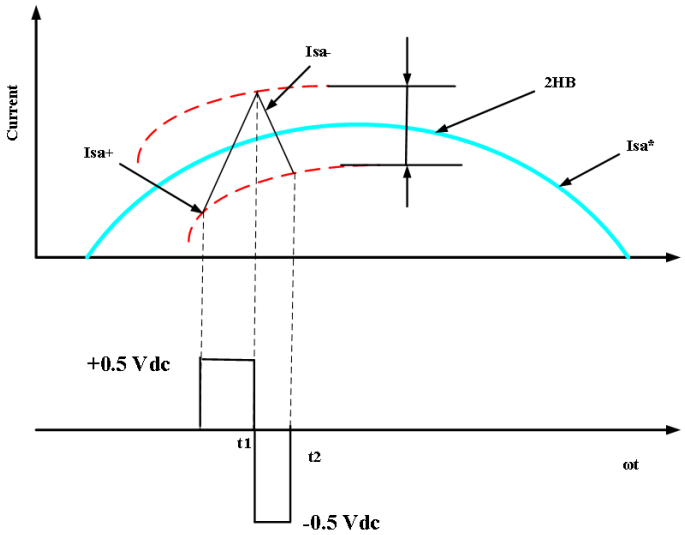

Fig. 15: AHCC switching scheme.

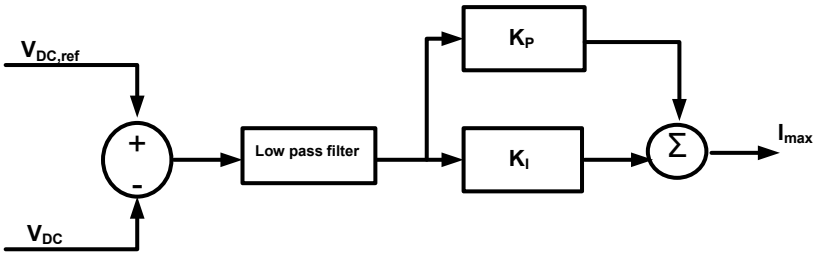

Fig. 16: PI controller.

reactive power. This scheme uses PI and FLC-based V_{dc} regulation as presented in the following section.

4.3.1 PI controller

The classic PI controller is typically used to manage the V_{dc} in the SAPF. Maintaining a steady V_{dc} is essential for achieving the desired SAPF compensating performance. If the active power is reduced to the point where the converter is unable to compensate for its losses, the active power will not remain constant. The measured V_{dc} is compared to the $V_{dc,ref}$, as shown in Fig. 16. With the use of PI controller parameters K_p and K_i, the PI controller regulates the generated error.

4.3.2 Fuzzy logic controller

The purpose of implementing the FLC is to maintain a constant dc-link voltage with minimum ripple. The FLC is characterized as follows.

- The triangular membership function is used for simplicity.
- A Mamdani-type min-operator for implication.
- Defuzzification using the centroid method.

The fuzzy sets for input and output variables in Table 2 are as follows. NB: Negative Big, NM: Negative Medium,

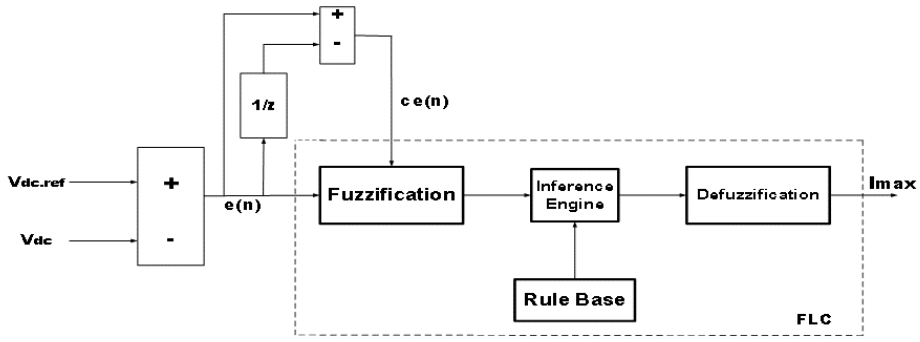

***Fig. 17**: Fuzzy logic controller.*

***Table 2**: Fuzzy rules.*

	$ce(n)$						
$e(n)$	NB	NM	NS	ZE	PS	PM	PB
NB	NB	NB	NB	NB	NM	NS	ZE
NM	NB	NB	NB	NM	NS	ZE	PS
NS	NB	NB	NM	NS	ZE	PS	PM
ZE	NB	NM	NS	ZE	PS	PM	PB
PS	NM	NS	ZE	PS	PM	PB	PB
PM	NS	ZE	PS	PM	PB	PB	PB
PB	ZE	PS	PM	PB	PB	PB	PB

NS: Negative Small, ZE: Zero Error, PS: Positive Small, PM: Positive Medium, and PB: Positive Big.

The dc-link capacitor voltage V_{dc} is sensed and compared with the reference voltage $V_{dc,ref}$. The error signal $e_n = V_{dc,ref} - V_{dc}$ and the change in error signal are used as input to the fuzzy processing as shown in Fig. 17.

The FLC computes the magnitude of the peak reference current I_{max}. I_{max} takes care of losses and the active power balance in the system. At the fuzzification stage, the numerical variables are transformed into linguistic variables. According to rules, inputs are processed by an inference mechanism to produce a suitable fuzzified output. This refers to the process by which the fuzzified outputs are converted back to the numerical values or control signal. The FLC is more widely used in active power filters than conventional controllers due to its better performance.

5. RESULTS ANALYSIS

Fig. 18 shows the proposed hybrid DG integrated with the SAPF. The performance of the proposed approach is examined in a variety of scenarios, as outlined below.

a) Scenario 1: Evaluation of performance under various nonlinear loads without the SAPF.

b) Scenario 2: Comparative performance analysis between the SRF-PI-HCC and MSRF-PI-AHCC schemes.

c) Scenario 3: Comparative performance analysis between the MSRF-PI-AHCC and proposed MSRF-FLC-AHCC scheme.

5.1 Analysis under Scenario 1

Under Scenario 1, the model simulated with an inductive/capacitive type nonlinear load without connecting the SAPF and the source current waveform with the harmonic spectrum are presented in Figs. 19(a) and 19(b) for the inductive case and Figs. 20(a) and 20(b) for the capacitive case, respectively.

It can be observed from Figs. 19(a) and 19(b) that the source current waveform is distorted with a typically high THD value of typically around 26.74%. Similarly, the source current for a capacitive load is also distorted or non-sinusoidal, with a THD of typically 20.25%, as shown in Figs. 20(a) and 20(b), respectively, according to the FFT analysis.

5.2 Analysis under Scenario 2

Under Scenario 2, the SAPF-based (using SRF-PI-HCC) control scheme is turned on to create a sinusoidal source current. The compensating current injected at the PCC point is shown in Fig. 21(a). As a consequence, the THD level drops to 3.52% as shown in Fig. 21(c), while the source current waveform becomes almost sinusoidal as shown in Fig. 21(b). Similarly, the comparable waveforms for the capacitive load are given in Figs. 21(d) to 21(f). The compensatory current created by the SAPF is illustrated in Fig. 21(d), reducing the THD level to 3.40% as seen in Fig. 21(f).

As can be observed from the V_{dc} waveform shown in Figs. 21(g) and 21(h), the ripples in the V_{dc} waveform are

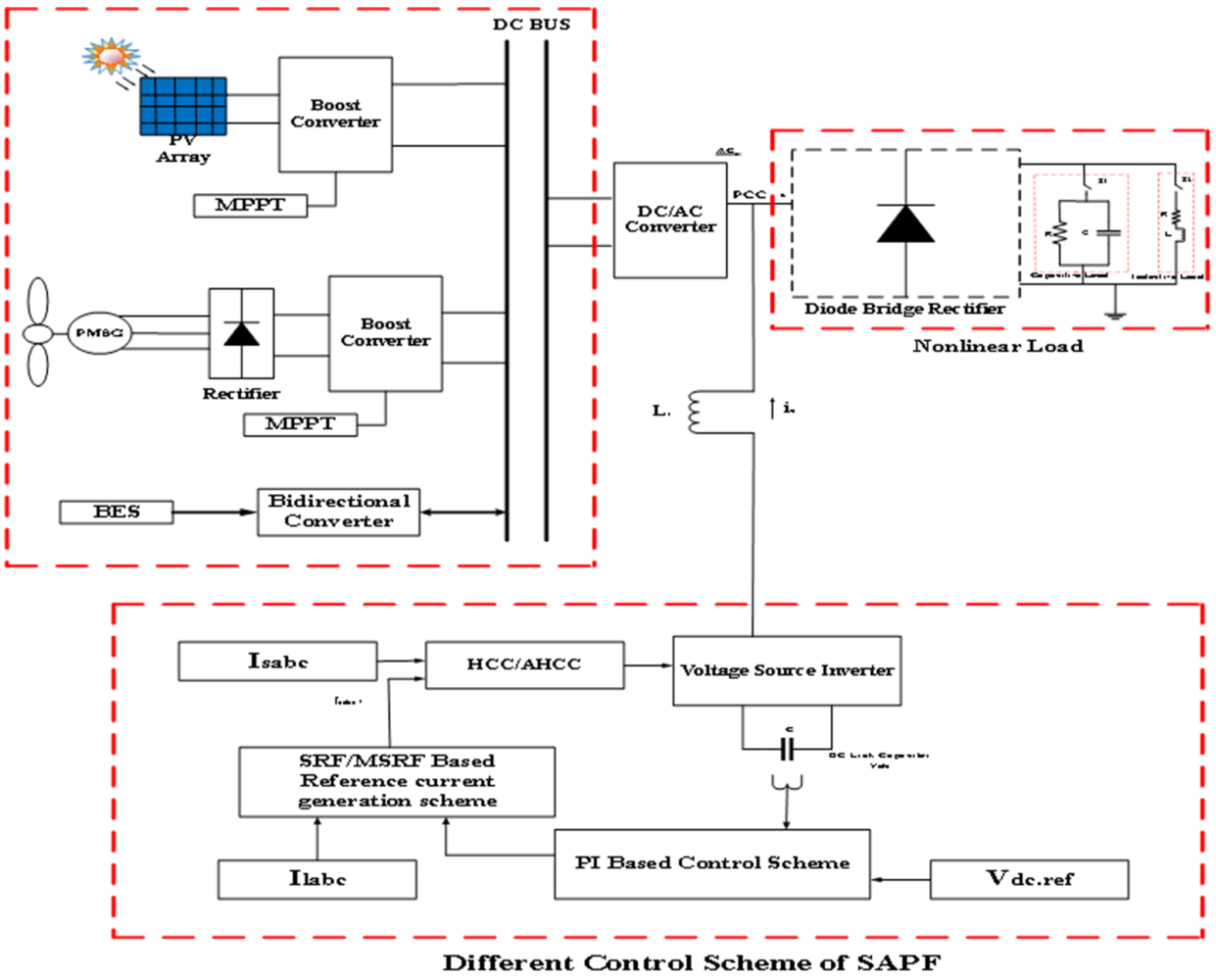

Fig. 18: Proposed system.

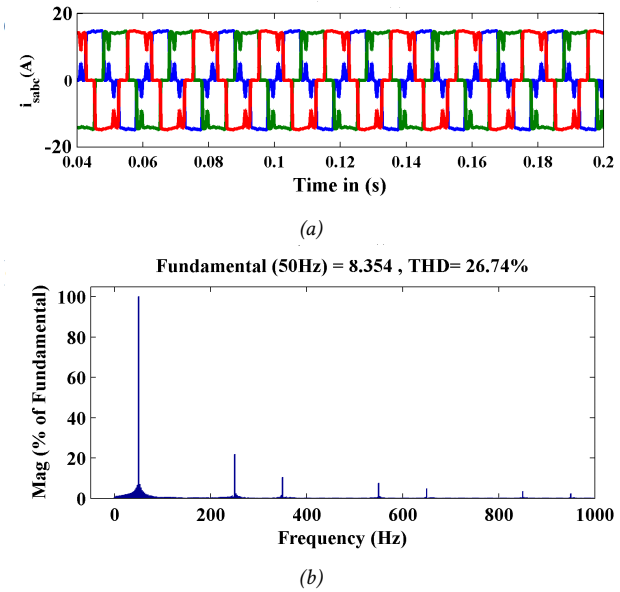

Fig. 19: Inductive load (a) i_s without SAPF (b) THD of i_s.

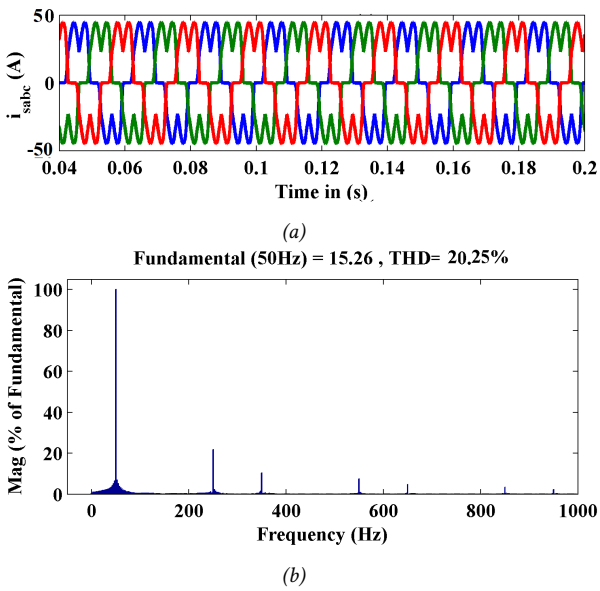

Fig. 20: Capacitive load (a) i_s without SAPF (b) THD of i_s.

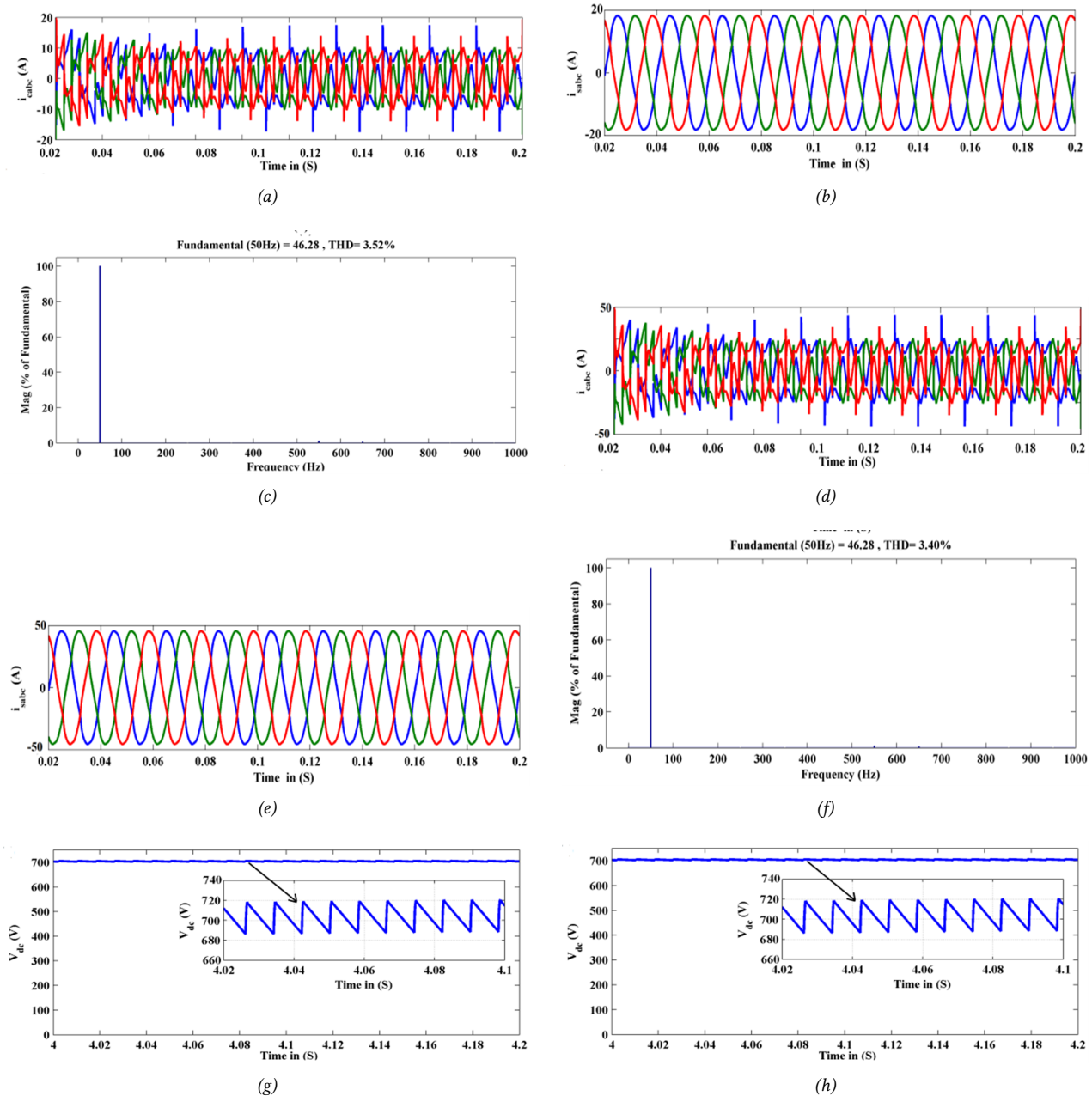

Fig. 21: *SAPF with SRF-PI-HCC scheme-based compensation; (a) i_c (inductive case), (b) i_s inductive case after compensation, (c) THD level (inductive case), (d) i_c (capacitive case), (e) i_s capacitive case after compensation, (f) THD level (capacitive case), (g) V_{dc} waveform for the inductive case, and (h) V_{dc} waveform for the capacitive case.*

nearly 20 V in both cases. However, the study reveals that there is a scope for a further reduction in the source current THD and ripples in the V_{dc} waveform. Hence, the SAPF is tested in a similar way using the MSRF-PI-AHCC control scheme. The waveforms for inductive and capacitive loads are shown in Figs. 22(g) and 22(h), respectively.

It can be seen from the figures that the THD is reduced to 2.32% and 2.18% for the inductive and capacitive load cases, respectively. Moreover, the ripples in the V_{dc} waveform are reduced to almost 8 V in both cases. Hence, it is clear from the study that the SAPF shows superior performance with the MSRF-PI-AHCC-based control scheme.

5.3 Analysis under Scenario 3

Owing to the drawbacks of the PI controller, it can be concluded that there is still scope for a further reduction in the THD source current and ripples in the V_{dc} waveform. Hence, the proposed controller in Scenario 3 is similarly tested using the proposed MSRF-FLC-AHCC control scheme. The V_{dc} waveforms for inductive and capacitive loads are shown in Figs. 23(g) and (h), respectively.

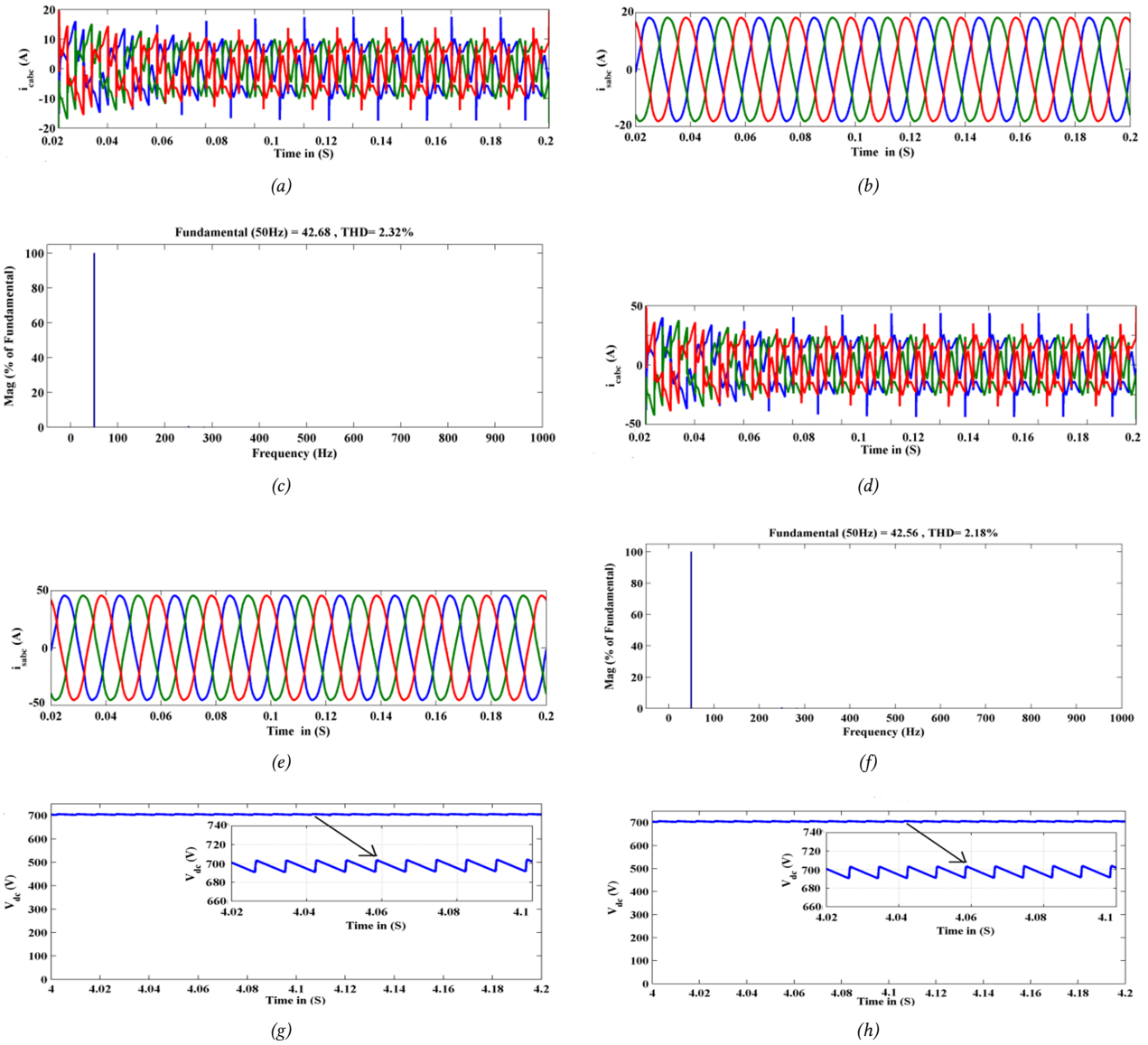

Fig. 22: *SAPF with MSRF-PI-AHCC scheme-based compensation; (a) i_c (inductive case), (b) i_s inductive case after compensation, (c) THD level (inductive case), (d) i_c (capacitive case), (e) i_s capacitive case after compensation, (f) THD level (capacitive case), (g) V_{dc} waveform for the inductive case, and (h) V_{dc} waveform for the capacitive case.*

As can be seen from the figures, the THD is reduced to 1.85% and 1.73% for the inductive and capacitive load cases, respectively. Moreover, the ripples in the V_{dc} waveform are reduced to almost 4 V for both cases. Hence, it is clear from the study results that the SAPF with the MSRF-FLC-AHCC-based control scheme demonstrates superior performance and good robustness. If the compensating current used is from $t = 0$ to 0.2 s then it can clearly be observed that the source current waveform is sinusoidal for both loads.

Table 3 summaries the analysis under three scenarios.

6. CONCLUSION

Harmonics in a hybrid power system (HPS) consisting of solar and wind energy are investigated in this study by integrating the proposed controller-based SAPF under different loading conditions. According to the results of experiments conducted in a MATLAB/SIMULINK environment, it can be observed that the proposed controller-based SAPF performs exceptionally well in mitigating the harmonics and reducing the dc-link voltage ripple under different load conditions. Based on a numerical comparison of the findings, the proposed controller-based (MSRF-FLC-AHCC) SAPF can reduce the source current harmonics by around 1.82% and 1.73% and ripples in the V_{dc} waveform to almost 4 V for inductive and capacitive loading, respectively. The THD levels and dc-link voltage ripple are within the permissible limits set by IEEE-519. Thus, the performance of the filter is satisfactory under steady state and dynamic loading conditions.

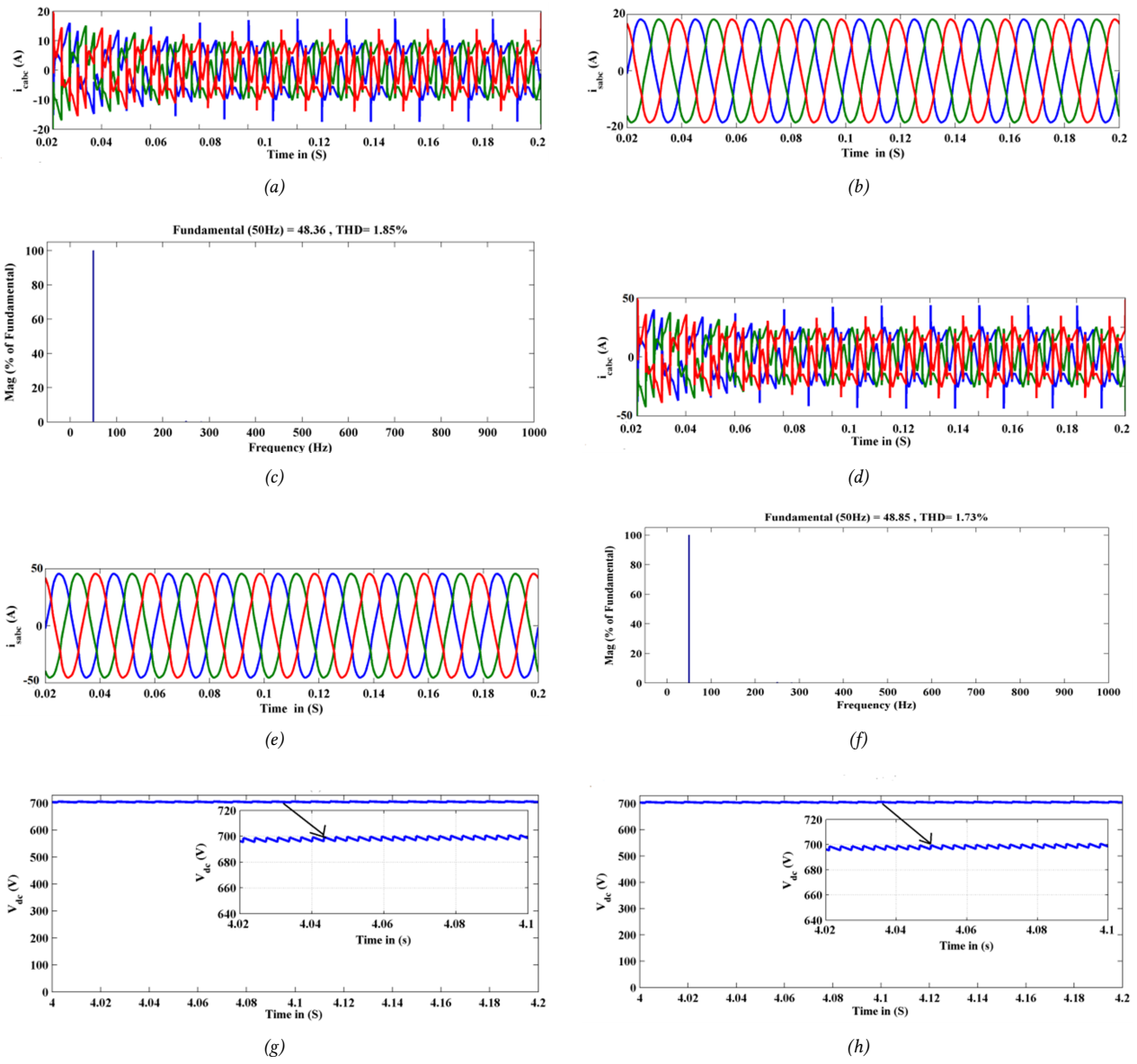

Fig. 23: *SAPF with MSRF-PI-AHCC scheme-based compensation; (a) i_c (inductive case), (b) i_s inductive case after compensation, (c) THD level (inductive case), (d) i_c (capacitive case), (e) i_s capacitive case after compensation, (f) THD level (capacitive case), (g) V_{dc} waveform for the inductive case, and (h) V_{dc} waveform for the capacitive case.*

Table 3: *Performance comparison.*

Controller	THD (without APF)	THD (with APF)	V_{dc} ripple
SRF-PI-HCC	26.74% (inductive load) 20.25% (capacitive load)	3.52% (inductive load) 3.40% (capacitive load)	20 V
MSRF-PI-AHCC	26.74% (inductive load) 20.25% (capacitive load)	2.32% (inductive load) 2.18% (capacitive load)	8 V
MSRF-FLC-AHCC	26.74% (inductive load) 20.25% (capacitive load)	1.82% (inductive load) 1.73% (capacitive load)	4 V

REFERENCES

[1] L. Suganthi and A. Williams, "Renewable energy in india — a modelling study for 2020–2021," *Energy Policy*, vol. 28, no. 15, pp. 1095–1109, Dec. 2000.

[2] S. R. Sinsel, R. L. Riemke, and V. H. Hoffmann, "Challenges and solution technologies for the integration of variable renewable energy sources—a review," *Renewable Energy*, vol. 145, pp. 2271–2285, Jan. 2020.

[3] J. Jurasz, F. Canales, A. Kies, M. Guezgouz, and A. Beluco, "A review on the complementarity of renewable energy sources: Concept, metrics, application and future research directions," *Solar Energy*, vol. 195, pp. 703–724, Jan. 2020.

[4] Y. Zhang, J. Ren, Y. Pu, and P. Wang, "Solar energy potential assessment: A framework to integrate geographic, technological, and economic indices for a potential analysis," *Renewable Energy*, vol. 149, pp. 577–586, Apr. 2020.

[5] P. K. Pathak, A. K. Yadav, and P. A. Alvi, "Advanced solar MPPT techniques under uniform and non-uniform irradiance: A comprehensive review," *Journal of Solar Energy Engineering*, vol. 142, no. 4, Aug. 2020, Art. no. 040801.

[6] O. Kuik, F. Branger, and P. Quirion, "Competitive advantage in the renewable energy industry: Evidence from a gravity model," *Renewable Energy*, vol. 131, pp. 472–481, Feb. 2019.

[7] D. Gielen, F. Boshell, D. Saygin, M. D. Bazilian, N. Wagner, and R. Gorini, "The role of renewable energy in the global energy transformation," *Energy Strategy Reviews*, vol. 24, pp. 38–50, Apr. 2019.

[8] B. Yang, T. Yu, H. Shu, Y. Han, P. Cao, and L. Jiang, "Adaptive fractional-order PID control of PMSG-based wind energy conversion system for MPPT using linear observers," *International Transactions on Electrical Energy Systems*, vol. 29, no. 1, Jan. 2019, Art. no. e2697.

[9] S. Samal, P. K. Hota, and P. K. Barik, "Performance improvement of a distributed generation system using unified power quality conditioner," *Technology and Economics of Smart Grids and Sustainable Energy*, vol. 5, 2020, Art. no. 24.

[10] S. Samal and P. K. Hota, "Design and analysis of solar PV-fuel cell and wind energy based microgrid system for power quality improvement," *Cogent Engineering*, vol. 4, no. 1, 2017, Art. no. 1402453.

[11] B. Singh, K. Al-Haddad, and A. Chandra, "A review of active filters for power quality improvement," *IEEE Transactions on Industrial Electronics*, vol. 46, no. 5, pp. 960–971, Oct. 1999.

[12] S. Samal, P. K. Hota, and P. K. Barik, "Harmonics mitigation by using shunt active power filter under different load condition," in *2016 International Conference on Signal Processing, Communication, Power and Embedded System (SCOPES)*, Paralakhemundi, India, 2016, pp. 94–98.

[13] A. Nassif, W. Xu, and W. Freitas, "An investigation on the selection of filter topologies for passive filter applications," *IEEE Transactions on Power Delivery*, vol. 24, no. 3, pp. 1710–1718, Jul. 2009.

[14] R. Davoodnezhad, D. G. Holmes, and B. P. McGrath, "A novel three-level hysteresis current regulation strategy for three-phase three-level inverters," *IEEE Transactions on Power Electronics*, vol. 29, no. 11, pp. 6100–6109, Nov. 2014.

[15] O. Bamisile, Q. Huang, J. Li, M. Dagbasi, A. D. Kemena, M. Abid, and W. Hu, "Modelling and performance analysis of an innovative CPVT, wind and biogas integrated comprehensive energy system: An energy and exergy approach," *Energy Conversion and Management*, vol. 209, Apr. 2020, Art. no. 112611.

[16] P. K. Pathak and A. K. Yadav, "Design of battery charging circuit through intelligent MPPT using SPV system," *Solar Energy*, vol. 178, pp. 79–89, Jan. 2019.

[17] A. O. Baba, G. Liu, and X. Chen, "Classification and evaluation review of maximum power point tracking methods," *Sustainable Futures*, vol. 2, 2020, Art. no. 100020.

[18] Y. Ouberri, H. Yatimi, and E. Aroudam, "Design of a robust sliding mode controller for MPPT based on automation PLC for PV applications," *International Transactions on Electrical Energy Systems*, vol. 30, no. 4, Apr. 2020, Art. no. e12296.

[19] S. Samal, P. K. Hota, and P. K. Barik, "Power quality assessment of a solar PV and fuel cell-based distributed generation system using unified power quality conditioner," *International Journal of Ambient Energy*, vol. 43, no. 1, pp. 3294–3304, 2022.

[20] P. K. Barik, G. Shankar, and P. K. Sahoo, "Power quality assessment of microgrid using fuzzy controller aided modified SRF based designed SAPF," *International Transactions on Electrical Energy Systems*, vol. 30, no. 4, Apr. 2020, Art. no. e12289.

[21] P. K. Barik, G. Shankar, and P. K. Sahoo, "DC-link capacitor voltage stabilization of a shunt active power filter using fuzzy logic controller under dynamic loading condition," in *Proceedings of Symposium on Power Electronic and Renewable Energy Systems Control*, S. Mohapatro and J. Kimball, Eds. Singapore: Springer, 2021, pp. 403–414.

[22] T. M. T. Thentral, K. Vijayakumar, S. Usha, R. Palanisamy, T. S. Babu, H. H. Alhelou, and A. Al-Hinai, "Development of control techniques using modified fuzzy based SAPF for power quality enhancement," *IEEE Access*, vol. 9, pp. 68 396–68 413, 2021.

[23] S. Mikkili and A. K. Panda, "PI and fuzzy logic controller based 3-phase 4-wire shunt active filters for the mitigation of current harmonics with the I_d-I_q control strategy," *Journal of Power Electronics*, vol. 11, no. 6, pp. 914–921, Nov. 2011.

[24] S. Mikkili and A. K. Panda, "Simulation and real-time implementation of shunt active filter i_d–i_q

control strategy for mitigation of harmonics with different fuzzy membership functions," *IET Power Electronics*, vol. 5, no. 9, pp. 1856–1872, Nov. 2012.

[25] A. K. Panda and S. Mikkili, "FLC based shunt active filter (p–q and I_d–I_q) control strategies for mitigation of harmonics with different fuzzy MFs using MATLAB and real-time digital simulator," *International Journal of Electrical Power & Energy Systems*, vol. 47, pp. 313–336, May 2013.

Pritam Patel received his B.Tech (EEE) from Biju Patnaik University of Technology, Rourkela, Odisha, India in 2012 & M.Tech (Power Electronic & Drives) from National Institutes of Technology Agartala, Tripura, India in 2015. He has completed PGDC in Thermal Power Plant from National Power Training Institute, Nagpur, India in 2016. He is pursuing his Ph.D. in Kalinga Institute of Industrial Technology, Bhubaneswar, Odisha, India. He has 6 years of industrial experience in aluminum industry, thermal power plant, high voltage substation & transmission line. His area of interest includes active power filter, power quality improvement, renewable energy.

Sarita Samal received her Ph.D. in Electrical Engineering from Veer Surendra Sai University of Technology, Burla, India in 2019, she did her M.Tech in power system engineering from Veer Surendra Sai University of Technology, Burla, India in 2006 and B.Tech (Hons) in Electrical Engineering from Berhampur University, India in 2003. She is currently working as an Assistant Professor-II in School of Electrical Engineering, Kalinga Institute of Industrial Technology deemed to be University, Bhubaneswar, Odisha. Her current research interests include power quality, renewable energy sources and microgrid. She has more than 45 numbers of research papers in international journal and conferences. She has published 6 book chapters in Elsevier, Taylor&Francis, and 5 patents.

Chitralekha Jena received her Ph.D. from Jadavpur University, Kolkata, India in 2017. She is working as Assistant Professor in School of Electrical Engineering since 2012. Her research are optimization of different power system using meta heuristics techniques, power management of smart grid, load frequency control, improvement of power quality using energy storage device. She has got best paper award from Institution of Engineers in 2017. She has published papers in 15 referred journal including Scopus and SSCI/CIE indexed journal, 32 papers in international conferences and 5 book chapter. She has organised two IEEE international conference. She is reviewer of many peer-reviewed Scopus/Web of Science indexed journals. She has published 5 patents. Out of which two are international patent. One Indian Patent and two International Patent has been granted. She has one project accepted by one multi-national industry. She was one of the evaluators for TOYCATHON-2021 organised Ministry of Education's Innovation Cell and AICTE, Government of India. She is also serving as the Counsellor, Youth Red Cross in the University since 2018.

Prasanta Kumar Barik received his B.Tech in electrical engineering from Utkal University, Odisha, India in 2005 and M.Tech. in Power Electronics and Drives from Kalinga Institute of Industrial Technology University, Odisha, India in 2009. He is currently pursuing his Ph.D. degree with the Department of Electrical Engineering at Indian Institute of Technology (Indian School of Mines), Dhanbad, India. He started his teaching career as a Lecturer with the Department of Electrical Engineering, C.V. Raman College of Engineering, Odisha, India, in 2006. He worked as an Assistant Professor with the Department of Electrical Engineering, Shiksha 'O' Anusandhan University, Odisha, India, from 2010 to 2012. He joined Odisha University of Agriculture and Technology (OUAT), India in 2012, where he is currently working as an Assistant Professor with the Department of Mechanical and Electrical Engineering. His current research interests include power quality improvement and application of power electronics with non-conventional energy sources and microgrid.